Projectile Impact Testing of Ice Hockey Helmets: Headform Kinematics and Dynamic Measurement of Localized Pressure Distribution.

Ryan Ouckama, David J. Pearsall

Abstract Ice hockey pucks are rubber projectiles that can carry >180 J of kinetic energy during a slap shot. When striking the temporal region of the skull, pressures capable of fracture can occur. Despite this risk, there is very little research on the topic. In this study, five helmet models, representing various material and shell compositions, were fit to a Hybrid III headform and subjected to puck impact at 24.2 m/s (PI_{24}) and 33 m/s (PI_{33}). The linear and angular kinematics of the headform and dynamic load distribution at the contact site were measured using 9 accelerometers and 25 force sensors. The cumulative strain damage measure (CSDM) was calculated using the SIMon (Simulated Injury Monitor) brain model. Thick-shelled HDPE helmets using different EPP foams tended to perform similarly, whereas the combination of thin polycarbonate shell and lightweight foam performed poorly, particularly at PI_{33}, for both acceleration-derived values and CSDM. Helmets with VN liners appeared to exhibit reduced CSDM as compared to models with EPP liners or a plastic cylinder array. The quantification of this impact type provides insight into current helmet effectiveness during this impact modality which may place players at risk of mTBI injury or scalp lacerations.

Keywords Ice Hockey, Helmet, Impact, Injury.

I. INTRODUCTION

Mandatory helmet use and the establishment of national safety standards were introduced to the sport of ice hockey following public outcry due to the high frequency of severe head injuries in the sport during the 1960s and 1970s. These injuries were caused primarily by blunt force trauma to the player's cranium (contact with ice, boards, puck, other players, etc.) resulting in skull fracture and cranial hematoma. Consequently, helmets were adopted in the sport to shield the head from mechanical distress and to reduce high magnitude localized loads on the skull [1]. Correspondingly, ice hockey helmet standards were established wherein the fundamental collision tests evaluate a helmet's capacity to limit peak linear acceleration below 275g for a vertical drop of a helmeted headform [2-4]. Modern helmets designed to these criteria have largely eliminated the incidence of blunt force trauma [5-6]; however, the high incidence of diffuse brain injuries such as concussions (herein referring to mild traumatic brain injuries or mTBI) remains a major concern.

The inability to obtain direct mechanical measures of cerebral tissue stress (and distress) response due to impact has been a major obstacle to understanding the etiology of mTBI. A promising alternative has been to use finite element analysis (FEA) of the brain and its tissues to estimate the stress and strain wave propagation resulting from cranial impacts that, in turn, correspond to brain injury risks. Using this approach, researchers have determined that measures of peak linear and angular acceleration alone do not correlate well to mTBI injury parameters [7]. Alternatively, the shape of loading curve inputs has been found to greatly influence the magnitude and distribution of principal strain and Von Mises stress values in FEA of the brain [8] and are substantially affected by the helmet's material and construction properties. Hence, the manner of force transmission within the local dynamic boundary of helmet/cranium contact site may greatly modulate the level of brain injury risk.

The potential to map local contact dynamics was demonstrated when Bishop and Arnold [9] investigated various ice hockey helmets' ability to distribute force during puck impacts to the temple region of a Hodgsen-WSU headform. This was accomplished by the use of pressure sensitive contact films placed between the headform and helmet at the site of puck impact. Their results showed that none of the helmet models tested were capable of managing the focal forces transmitted to the temporal region. Though headform global accelerations were below 275g, substantial pressure magnitudes (>5MPa) were achieved. Since the pressure films provided only a summative picture of the impact event, the temporal history was lost. The authors noted

R. Ouckama is an NSERC Industrial Research and Development Post-Doctoral Fellow at Bauer Hockey Corp. St-Jerome, Quebec, Canada (450-436-2292 x457, ryan@ouckama.com). D. J. Pearsall is a Professor in the Department of Kinesiology and Physical Education, McGill University in Montreal, Canada.

that further exploration of load measurement techniques and appropriate thresholds were needed. Current developments in flexible force sensor arrays make possible accurate spatial and temporal mapping of foam impact events [10]. Furthermore, these sensor arrays have been shown to function well in standardized linear helmet drop tests [11]. These sensor arrays provided gross estimates of headform acceleration comparable to that of the accelerometer, yet also were able to discriminate spatial contact differences between helmet models. This latter observation is most relevant, as it offers the potential to quantify the input characteristics needed for realistic finite element modeling of impact behavior. Further study using this testing technique is thus warranted.

In this vein, this study extends the use of force sensor arrays to examine puck projectile impact events to ice hockey helmets. In a typical vertical drop test, the headform falls at a low speed onto a static anvil (i.e. high-mass, low-velocity impact), whereas in the projectile test, the puck moves at high speed on the static headform (i.e. low mass, high-velocity impact). These impact types are typical of collision events in the game of ice hockey [12]; yet, few studies have examined projectile impacts to ice hockey helmets [13-14]. The kinetic energy of a projectile puck impact can easily exceed the energy levels established in the helmet standards. For example, an official 160g hockey puck must travel at only 24.2 m/s to impact a helmet with 47J of kinetic energy, equal to the impact energy during drop testing of medium-sized helmets in the CSA ice hockey helmet standard (CSA z262.1-09). Professional hockey players can achieve puck velocities of up to 48 m/s during a slap shot [15], reaching kinetic energy (184J) levels nearly 4 times that of the linear drop test. Considering the potential of puck-to-helmet impact for higher energy, shorter contact duration and a smaller contact area, there is potential for significantly greater levels of helmet material deformation and stress during this impact modality relative to traditional helmet testing methods. Given the lack of data for measures of linear and angular acceleration as well as load distribution during these highly focal impacts, the authors propose to quantify these measures across a cross section of several commercial ice-hockey helmet models, representing various material types and geometries, and assess their performance during puck impact events while attempting to identify any construction properties that may perform favorably.

II. METHODS

A 50th percentile Hybrid III dummy headform (Model 78051-61X-1846, Humanetics Innovative Solutions, Inc., Plymouth, MI) and Hybrid III neck (Model 78051-90) were fitted with multiple accelerometers and force sensors. Linear and angular acceleration variables were collected using a 3-2-2-2 orthogonal array [16-17] of 9 linear accelerometers (Model 7264C-500, Meggitt's Endevco, San Juan Capistrano, CA). Load distribution was measured by instrumentation of the dummy forehead with 25 discrete flexible force sensors (Flexiforce® model A201, Tekscan, USA). The sensor voltage output was calibrated to force using a gold-standard piezoelectric force plate as a simultaneous signal reference (Kistler 925M113 with Model 5015 Charge amplifier). A drop method presented in earlier work by Ouckama and Pearsall [10-11] was utilized to simulate high impact loading rates and verify the flexible force sensor response time during short duration impact. A 5×5 grid, corresponding to wireframe intersections of the Hybrid III finite element (FE) model (LS PrePost 4.1, LSTC, Livermore, CA) was transferred to the physical headform (Figure 1). The grid was symmetrical about the median plane with spacing of 2-3 wireframe intersections to provide room for the Flexiforce® sensors on the physical headform. Two reference points on the FE model were established (tip of nose and 6.4 cm superior of nose along the median plane). Linear measures between the reference points and each grid location were recorded using LS-PrePost 4.1 software. A drafting compass was then used to transfer the grid coordinates to the physical Hybrid III head by intersecting arcs of fixed distances from the reference points. This method of sensor placement was developed to allow future comparisons between the empirically measured forces and the contact stresses predicted by corresponding FE analysis with modeled helmets. The force sensors were adhered directly to the headform using double-sided tape. Care was taken to minimize overlap of the sensors and cabling. A nylon stocking was placed over the instrumented headform to minimize shear forces, and to mimic the movement of human skin beneath the helmet [18]. Two 32-channel analog acquisition modules (NI-9205, National Instruments, Austin, TX) were installed in a CompactDAQ chassis (cDAQ-9174). One module, operating at 20 KHz, was dedicated to capture of the 9 head accelerometers, while the second, operating at 10 KHz captured the 25 analog force channels. Synchronization between the channels was maintained by a common timing engine within the CompactDAQ chassis. Accelerometer channels were conditioned by three, 3-channel amplifiers (Model 136, Meggitt's Endevco, San Juan, CA) each employing a CFC1000 hardware anti-alias filter

[19]. The Flexiforce® sensors were conditioned using custom hardware based on the recommended MCP-6000 series op-amp [20]. Accelerometer and force data were post-processed in MATLAB® (r2012 ,The MathWorks, Natick, MA) using a digital Butterworth filter meeting CFC1000 specifications. Force measures at each sensor were converted to pressure based on the active sensor area (0.71 cm^2) and then using the physical sensor coordinates, interpolated to a matrix of 50×50 pressure sensels using a MATLAB script.

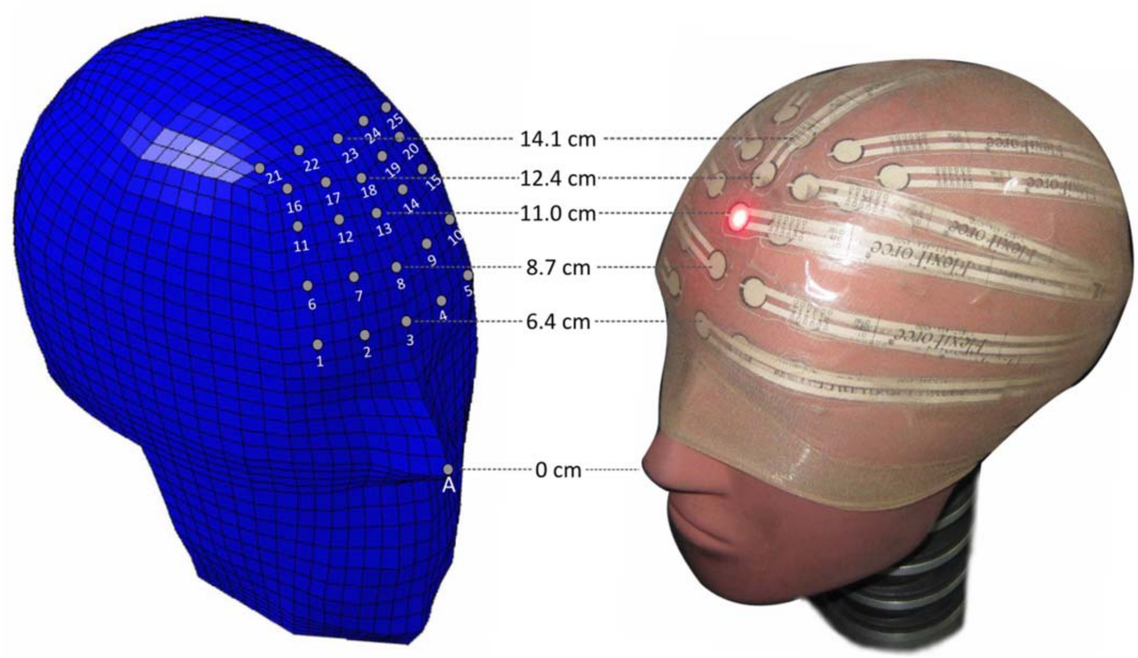

Figure 1: Force sensor locations (25) were selected based on wireframe intersections of the Hybrid III finite element model (left). The virtual coordinates were transferred to the physical headform (right). The point-to-point distance from reference point A (tip of nose) to each sensor row along the median plane is displayed. A red laser on the physical headform indicates the alignment of the projectile canon with the central sensor.

The head/neck assembly was mounted in a pneumatic ice hockey puck cannon fixture. The fixture allowed for the head to translate along the x-axis of the headform (fore-aft); however, this was locked in a stationary position for this experiement. Pilot testing showed no significant difference between peak acceleration values between the locked and free position as the base did not translate until after the impact event. The cannon fired a regulation ice hockey puck (mass=160 g) at ambient room temperature at a precise point on the headform 11cm superior of the tip of nose in the mid-sagittal plane (Point #13, Figure 1). Ten samples of five different models of hockey helmets, representing various material types and geometries, were obtained for the study (Table 1). For each model, 5 helmet samples were subjected to a 24.2 m/s puck impact (PI_{24}). This velocity was selected to provide approximately the same kinetic energy (47 J) as the linear impact test for medium-size hockey helmets [4]. An additional 5 samples for each model were then subjected to a puck impact at 33 m/s (PI_{33}) providing 87 J of kinetic energy. This velocity was selected as it is common to test the toughness of full-face protectors (i.e cage/shield) in various hockey helmet standards for projectile impact [2][21]. Both impact speeds represent shot speeds capable by a skilled hockey player (87 & 118 km/h). Time between impacts was between 60-90 seconds to allow for retrieval of the puck and pressurizing of the air canon. Puck velocity was measured by two laser light traps at the distal end of the cannon barrel.

The Simulated Injury Monitor (SIMon 3.07) was utilized to calculate corresponding stresses and strains of the brain tissue based on the 3-2-2-2 accelerometer array in the Hybrid III headform. This finite element model includes a rigid skull, cerebrum, celebellum, brainstem, ventricles, combined cerebrospinal fluid (CSF) and pia arachnoid complex layer, falx, tentorium and parasagittal blood vessels [22]. The model behavior is validated using data from relative motion of the brain [23] and intracranial stress during impact [24-25]. The model can be used to predict the likelihood of diffuse axonal injury (DAI) by way of a cumulative strain damage measurement (CSDM 0.25). The percentage of the brain model elements exceeding the 0.25 strain threshold is calculated over time and correlated to DAI based on scaled animal experiments [22]. These injuries can be classified using the Abbreviated Injury Scale (AIS), which describes the threat to life. While not developed specifically for mTBI, the scale can be used to classify this injury type. A mTBI with no loss of consciousness is considered AIS1 whereas diffuse axonal injury (DAI) involving diffuse damage to the axons of the brain is considered AIS 4-5. Previous work adapted the injury likelihood curve for DAI (AIS4+) to less severe AIS1+ injuries such as mTBI [26]. This metric was calculated based on the SIMon model CSDM 0.25 outputs.

Table 1: Physical characteristics of the five ice hockey helmet models evaluated in this study. Ten samples of each model were obtained. Manufacturer and model number data are excluded.

	Helmet 1	**Helmet 2**	**Helmet 3**	**Helmet 4**	**Helmet 5**
Liner Type	Perforated Vinyl Nitrile	EPP	EPP	EPP	Plastic cylinder array
Shell Type	Two-piece HDPE	Two-piece HDPE	Two-piece HDPE	One-piece polycarbonate	One-piece HDPE
Shell Thickness	2.3 mm	2.3 mm	2.3 mm	0.5 mm	2.5 mm
Mass (*n*=10)	557±5 g	514±1 g	578±4 g	322±5 g	609±4 g
Size	Medium	Medium	Medium	Medium	Medium

A factorial ANOVA (α=0.05) was calculated (Statistica v8.0, Statsoft, Inc, Tulsa, OK) for categorical predictors of puck velocity (2) and helmet model (5). Dependent measures of peak linear acceleration, peak angular acceleration, peak pressure, average pressure and AIS1+ injury risk were analyzed. Post–hoc analyses of significant factors were calculated using the Tukey-HSD test. Data exclusions occurred if puck velocity was greater than ±5% from the goal velocity, or a visible material failure resulted in abnormal acceleration curves.

III. RESULTS

The total number of trials for each helmet model is presented in Table 2. Of the 50 samples tested, a total of 34 helmets were included in statistical analysis following exclusion for impact velocity and helmet failure (cracking).

Table 2: Total number of impact trials per helmet model.

	Puck Velocity		
	24 m/s	33 m/s	Total
Helmet 1	3	3	6
Helmet 2	3	5	8
Helmet 3	3	3	6
Helmet 4	3	3	6
Helmet 5	3	5	8
Total	15	19	34

Average puck velocities were 24.2 ± 0.2 and 32.9 ± 0.6 m/s for impact conditions PI_{24} and PI_{33}. The average time for the headform to reach peak resultant acceleration (t_{acc}) across all helmet models was 1.28 ± 0.28 ms for 24 m/s puck impacts (PI_{24}) and 1.07 ± 0.10 ms at 33 m/s puck impacts (PI_{33}). After initial compression of the helmet materials, the puck typically rebounded at an elevated trajectory followed by rotation of the head by an average of 13.8 ± 1.1 degrees rotation during PI_{24} and 18.9 ± 2.2 degrees rotation during PI_{33} (Figure 2). Rotation angles were calculated by a double integration of the rotational acceleration about the medio-lateral y-axis of the head. Average time to maximal neck extension was 68.0 ± 2.4 ms for PI_{24} and 73.2 ± 2.6 ms for PI_{33}.

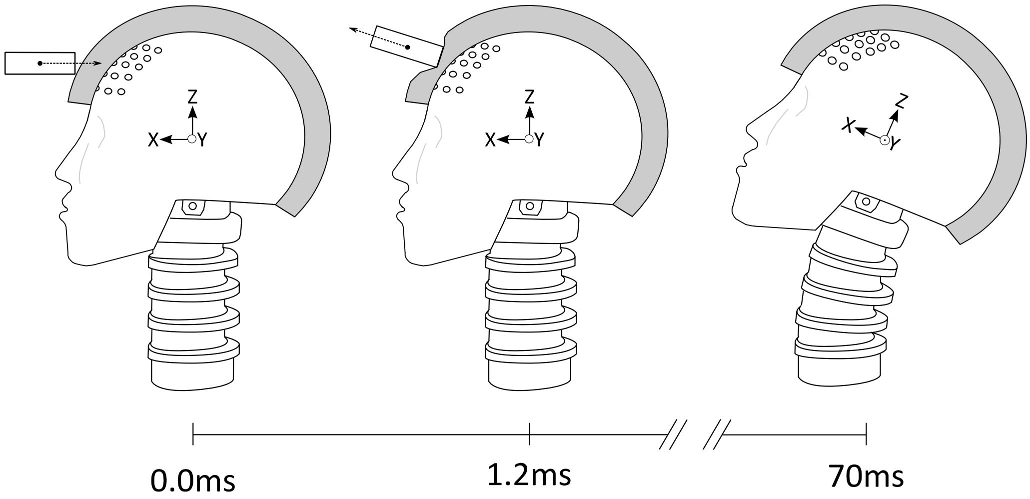

Figure 2: Event sequence for the impact of a 160 g hockey puck into a helmeted Hybrid III headform. The period over which the material can dissipate force is very brief (<2 ms) relative to a vertical drop test (~10 ms). Initial contact occurs at the lower leading edge of the puck due to the curvature of the helmet. The rotational displacement of the headform peaked around 70 ms.

The dependent measures of linear acceleration, angular acceleration, average pressure, peak pressure, injury risk (AIS1+) and CSDM 0.15 are presented for impacts to the five differing helmet models by an ice hockey puck at 24 m/s (Table 3) and 33 m/s (Table 4). Given the extremely low values of AIS1+ injury risk (based on CSDM 0.25), CSDM 0.15 was additionally reported.

Table 3: Average resultant linear acceleration, resultant angular acceleration, average pressure, maximal pressure, AIS1+ injury risk and CSDM 0.15 during impact to 5 models of ice hockey helmets by an official-sized puck travelling at 24.2 m/s. Maximal values are indicated by bold type. Data are mean (s.d.)

Helmet Model	Impact Velocity = 24.2 m/s						
	Linear Acc (g)	Angular Acc (rad/s^2)	Angular Vel. (rad/sec)	P_{avg} (N/cm^2)	P_{max} (N/cm^2)	Injury Risk AIS1+ (%)	CSDM 0.15 %
1	**62.4 (4.7)**	5423 (334)	6.4 (0.1)	**76.7 (4.5)**	**210.8 (11.0)**	<0.01	0.75 (0.10)
2	57.0 (2.3)	5043 (168)	6.7 (0.2)	66.3 (3.7)	186.8 (23.6)	<0.01	1.16 (0.24)
3	60.2 (2.5)	5185 (149)	7.2 (0.5)	70.8 (6.4)	186.6 (24.3)	<0.01	2.41 (0.77)
4	44.6 (4.9)	**5434 (408)**	**7.7 (0.2)**	59.8 (11.5)	132.7 (46.6)	<0.01	**3.08 (0.51)**
5	40.6 (3.5)	3645 (168)	6.8 (0.2)	64.7 (10.3)	181.1 (28.2)	<0.01	1.13 (0.13)
Average	53.0 (9.6)	4946 (727)	7.0 (0.5)	67.7 (8.9)	179.6 (36.1)	<0.01	1.71 (0.99)

Table 4: Average resultant linear acceleration, resultant angular acceleration, average pressure, maximal pressure, AIS1+ injury risk and CSDM 0.15 during impact to 5 models of ice hockey helmets by an official-sized puck travelling at 33 m/s. Maximal values are indicated by bold type. Data are mean (s.d.)

Helmet Model	Impact Velocity = 33 m/s						
	Linear Acc (g)	Angular Acc (rad/s^2)	Angular Vel. (rad/sec)	P_{avg} (N/cm^2)	P_{max} (N/cm^2)	Injury Risk AIS1+	CSDM 0.15 %
1	110.1 (9.4)	8538 (1074)	7.6 (0.2)	120.4 (10.7)	374.1 (43.7)	0.01 (0.00)	3.20 (0.59)
2	97.1 (4.3)	8742 (224)	8.8 (0.3)	100.9 (4.5)	353.0 (33.6)	0.03 (0.01)	5.82 (1.16)
3	96.7 (36.3)	7981 (3156)	8.1 (0.6)	97.9 (34.1)	344.6 (171.4)	0.02 (0.03)	5.14 (2.84)
4	**110.2 (7.4)**	**10281 (675)**	**10.7 (0.2)**	**127.5 (8.0)**	**521.4 (68.6)**	**0.39 (0.20)**	**14.36 (1.36)**
5	77.9 (8.7)	7604 (1220)	8.6 (0.5)	96.5 (10.7)	373.0 (60.2)	0.02 (0.01)	6.02 (1.69)
Average	96.1 (18.5)	8533 (1562)	8.8 (1.0)	106.5 (18.3)	386.9 (93.6)	0.08 (0.16)	6.70 (3.83)

There was a significant main effect of CSDM 0.15 for helmet model ($p<0.01$). Helmet model 1 (VN foam with HDPE shell) had the lowest CSDM values (1.97%) whereas model 4 (Light EPP foam with thin polycarbonate shell) had the highest CSDM result (8.7%) (Tukey HSD $p<0.05$). The remaining models consisting of thicker HDPE shells and with EPP or plastic cylinder array liner constructions performed similarly (CSDM 0.15=3.4-3.7%). Despite strengths of each particular material in singular metric of linear/angular acceleration, the overall effect of cumulative brain model strain was managed best by the thick-shelled VN construction. Individual dependent variables were correlated to CSDM values to see if any predictors might exist. Rotational velocity was found to be the highest correlate with CSDM (r=0.97), followed by rotational acceleration (r=0.81) and maximum contact pressure (r=0.80). Linear acceleration correlated relatively low to CSDM (r=0.67).

Flexible force sensor voltage correlated highly to load cell output during calibration (mean R^2= 0.997±0.001). Average RMSE values across the entire measurement range were 4.3±0.9 N. This represents approximately 2% error for peak forces over 200 N. As pressure data have not been presented before for this type of impact, the following section will focus on the load distribution properties of each helmet model. Visual plots of pressure distribution at peak-load and time-series data for each sensor are presented for PI_{24} (Figure 6) and PI_{33} (Figure 7) conditions.

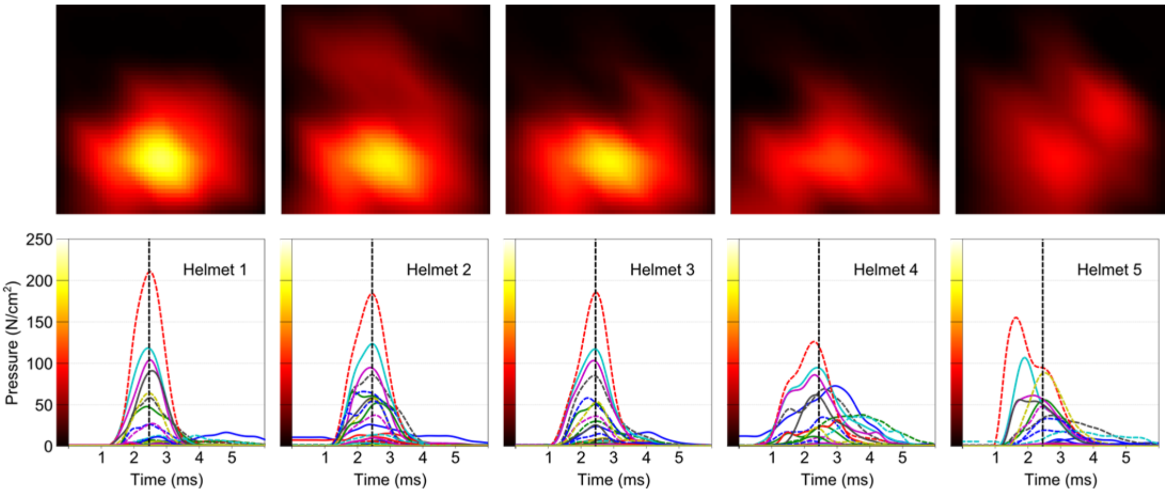

Figure 6: Low-speed sample trials showing spatial loading profiles between 5 differing helmet models during impact by a 160g hockey puck at 24 m/s. Twenty-five discrete force signals (lower panel) were recorded at the helmet-head interface of a Hybrid III headform. The dashed vertical line represents the instant of maximal net force. Pressure maps (upper panel) represent the spatial pressure distribution at this same instant.

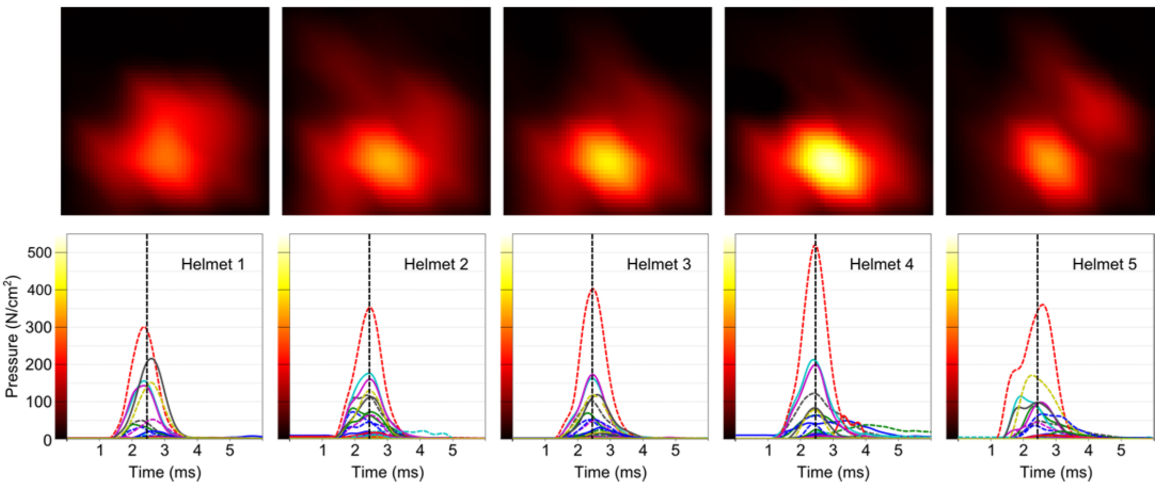

Figure 7: High-speed sample trials showing spatial loading profile between 5 differing helmet models during impact by a 160g hockey puck at 33 m/s. Twenty-five discrete force signals (lower panel) were recorded at the helmet-head interface of a Hybrid III headform. Vertical dashed lines represent the instant of maximal net force. Pressure maps (upper panel) represent spatial pressure distribution at this same instant.

The natural curvature of the forehead caused the lower leading edge of the puck to make first contact (see Figure 2 above) likely resulting in the non-centric pressure concentration. Time-series plots of the individual load sensors averaged across helmet replicates are presented below the corresponding pressure distribution plots. The foam-based helmets (Helmets 1-4) had similar loading profiles with a single rise to a central maximum. This was not true in Helmet 5, which does not utilize traditional padding materials. The resulting loading patterns were notably different from the other helmet types and displayed a rapid rise of the central sensor (red-dashed) followed by delayed onset of the remaining sensors which peaked at various different timings. Factorial ANOVA revealed no significant main effect for helmet model ($F_{4,24}$)=2.32,p=0.085 or the interaction of Model*Velocity (F(2,24)=2.49, p=0.07 for average contact pressure. For peak contact pressure there was a significant interaction effect of Model*Velocity ($F_{4,24}$)=3.58, p=0.01. The interaction effect was significant due to fact that helmet model 4 had the lowest peak pressure (132.7 N/cm^2) during PI_{24} and the highest peak pressure (521.4 N/cm^2) during PI_{33}.

IV. DISCUSSION

In similar sports to ice hockey involving projectile ball/puck and a stick (field hockey/lacrosse) the most common injury mechanisms are player-to-player contact (31%), followed by stick contact (27%), falls (18%) puck/ball (15%) and other (9%) [27]. Projectile puck impact to a player's head is a possible event during the game of ice hockey and can result in injuries including laceration, contusion, fracture and concussion [6][27]. Thus, it is important that athletes participating in ice hockey have adequate head protection from these highly focal impacts. Yet, despite this injury risk, remarkably little research has focused on the measurement of puck impacts to player helmets, particularly with regard to the forces generated. The purpose of this paper was to investigate the kinematics of this impact type in addition to surface-loading characteristics at the contact interface of the helmet and head during low-mass, high-velocity puck impacts.

Our results show that 33 m/s puck impacts can generate substantial linear and angular accelerations as well as localized contact forces sufficient for scalp injury. The majority of PI_{24} impacts resulted in linear and angular acceleration values below the proposed 50% injury thresholds for concussion, based on football data, of 82g and 5900 rad/s^2 [28]. However, at higher puck velocities (PI_{33}), easily achieved by skilled players, linear and angular accelerations exceeded 106g and 7900 rad/s^2, representing an 80% risk of mTBI injury [28]. These mTBI risk values must be interpreted very cautiously in this context, however, as they originate from longer duration head-to-head impacts from football datasets and human tolerance to acceleration is higher at shorter durations. Linear and angular acceleration results from puck impact were strongly correlated (r^2=0.85). The peak rotational acceleration values (4946±727 rad/s^2) obtained during PI_{24} were close in magnitude to a similar helmet population tested using a 7.5 m/s pneumatic linear impactor (4.9-5.9 krad/s^2) [29]. The average rotational acceleration during PI_{33} (8533±1562) rad/s^2) was in a range similar to that observed during a punch (hook) from an Olympic boxer (9300 ±4485 rad/s^2) [30]. The lowest average angular acceleration (average of mean helmet angular acceleration at PI_{24} and PI_{33}) was obtained for Helmet 5 (5624 rad/s^2) constructed using a thermoplastic impact-absorbing material whereas the greatest angular acceleration value (7858 rad/s^2) was observed from Helmet 4 utilizing a thin polycarbonate shell. During short-duration puck impact, we observed no significant differences in angular acceleration between helmet models using VN (Helmet 1) and EPP (Helmets 2-3) materials with similar HDPE shell. This result differed from testing using longer duration NOCSAE style linear impactor [31] where VN foam produced lower angular acceleration values than EPP constructions at 4 of 5 impact sites. However, when acceleration is integrated over time, angular velocity of the VN model (Helmet 1) was significantly lower than other models. Angular velocity was found to correlate highest (r^2=0.98) with principal strain measures (CSDM 0.15). This was also apparent in analysis of college football data for the correlation of angular velocity and CSDM 0.15 values (r^2=0.92) [22]. Additionally, CSDM FE model outputs were more sensitive to rotational components as opposed to linear components [32]. The high correlation with angular velocity and FE model cumulative strain underlines the importance of looking beyond simple comparisons of peak linear and angular acceleration values. Helmet model 4 had the highest linear, angular and CSDM results at PI_{33}, yet it had one of the lowest linear acceleration values at PI_{24}. This result may be attributed to the use of a soft shell and light-weight EPP liner. Using simulations, softer liners were calculated to perform optimally during low-speed impact; however, during higher speed impact, a stiffer liner was optimal for reduction of linear acceleration [33]. This simulation phenomenon was likely observed in this particular model. Given the considerable variance in liner stiffness between helmet models, material selection should be balanced for performance during both high-mass low-velocity and low-mass high-velocity type impacts (i.e., head drop and puck projectile tests, respectively) to protect the athlete from these foreseeable risks of the game. Pressures ranging from 285-544 N/cm^2 (2.85-5.44 MPa) were recorded during PI_{33}. These pressures were lower than Bishop's [9] side-impact results (8-20 MPa); however, this could be expected due to the thicker padding and uniform shell coverage at the front of the helmet in comparison to the temporal region. We avoided testing the temporal region due to large variance between helmet models in adjustment fixtures often located at the side of the helmet, the presence of shell overlap in 2-piece designs and variable geometry. The front site was deemed a more representative location to test the varying material types used in the helmet constructions with more constant geometry. Additionally, based on statistics of collegiate hockey player wearing instrumented helmets, the most likely site for impact was at the front (30%) and back (33%) of the head [34]. Puck-specific impact location statistics were unavailable. Relating pressure to skull fracture tolerance is challenging, as the literature typically reports fracture limits in net force despite the fact that often different impactor sizes and shapes are used. Part of the challenge in reporting tolerance limits in pressure is the inability to know the instantaneous contact region of the impactor. Frontal bone fractures were as low as 2670 N using a 6.45 cm^2 cylindrical impactor [35], which, if fully engaged with the bone surface, would be 4.1 MPa. In a more recent study, a projectile impact to the temporo-parietal bone was evaluated with an impactor of similar mass (103 g) and speed (33 m/s) to the ice hockey puck. A 50% risk of fracture was calculated at 4572 N over an area of 11.4 cm^2 (4.0 MPa) [36]. The average net force, calculated by the average pressure multiplied by total contact area, was 3425N during PI_{24} and 6175 N for PI_{33}. Given the total contact region was 51-61 cm^2 during helmeted impact, it is unlikely that there is any risk for fracture in this context. However, laceration could be possible with forces greater than 4000 N based on experiments on porcine subjects with impactors (shoe sole) of similar contact area [37].

The current study is unique from earlier work in the application of dynamic measures of load distribution and the inclusion of rotational kinematics. The synchronized measures permitted visualization of the changes in load distribution across time. Functional differences between helmets and impact tests could be identified. For example, the plots of contact pressure at PI_{24} (Figure 6) and PI_{33} (Figure 7) demonstrated the differences in material responses undetected by global force or acceleration measures. Helmets with the highest peak linear acceleration did not correspond to those with the highest peak pressures. Thus further site by site analysis of puck impact-induced pressure transmission is warranted, particularly at more vulnerable locations of the head. The assumption that shell/liners will uniformly transmit contact pressures was found to be untrue. For instance, during PI_{24} to Helmet model 5, load concentration was initially focused on a single central sensor and then yielded to multiple points away from this central sensor, perhaps as a function of the plastic engineered liner. Furthermore, this dynamic pressure mapping method identified unexpected differences in loci of point of contact to headform. For example, the incident location of the puck to the helmet's outer shell did not correspond to the liner/headform surface maximum location (Figures 6 and 7). Due to the curvature of the head, the load concentration occurred at the inferior leading edge of the puck (Figure 2). Without this mapping evidence, the difference between presumed and actual head impact location would not have been immediately apparent.

This study has several limitations. First, CSDM was presented at a lower principal strain threshold (0.15 vs. 0.25). CSDM 0.15 was more appropriate for the data presented as values ranged from approximately 1-15%. While CSDM 0.15 has been shown to correlate with concussion risk [38], it is not validated with animal data, which was calculated at CSDM 0.25. Despite this limitation, CSDM 0.15 correlates very highly with CSDM 0.25 (r^2=0.98) in this dataset. Second, the duration of impact data used to validate concussion outcomes (football) is typically longer (10-15 ms) than that of puck impacts to the head (1-2 ms). All results must therefore be interpreted cautiously. There is a need for injury validation at lower strain thresholds with respect to mTBI injuries using the SIMon FE model. Finally, the response of the Hybrid III neck is validated using passive motion of a human cadaver secured to a sled during a frontal crash [39]. Thus the neck motion resulting from projectile puck impact to the dummy head is not validated against a human data set. Although these data do not represent the exact response of a human head, they are repeatable and provide useful comparison with the growing literature base of sport-injury impact reconstructions using the Hybrid III headform.

V. Conclusions

Further research is warranted to assess the risks posed by short duration projectile impacts experienced in sports such as ice hockey, baseball, cricket and lacrosse. The measurement of load distribution during projectile impact provided useful data for identification of possible focal injury risks (e.g., laceration), and increased understanding of material behaviours and load concentrations caused during various impact modalities. Additionally, with the increasing application of finite element modelling to helmet optimization and head injury prediction, these data may serve to validate the corresponding contact stresses estimated by these models at the helmet-head interface. This initial study shows promising results in determining principal strain performance differences based on helmet material constructions; however, further work is needed to verify if the effect is repeatable and if the injury results are meaningful, especially given the short duration relative to typical head to head impacts that the majority of sports injury data is based upon.

VI. Acknowledgement

This research was supported by the Industrial Innovation Scholarship (IIS) in collaboration with the Fonds de Recherche du Québec – Nature et technologies (FRQNT), the Natural Science and Engineering Research Council of Canada (NSERC) and Bauer Hockey Corp.

VII. References

[1] Reid SE, Reid Jr. SE. Advances in sports medicine. Prevention of head and neck injuries in football. *Surg Annu*, 1981, 13:251–270.

[2] ISO. 10256:2003 Head and face protection for use in ice hockey. International Standards Organization, Geneva, Switzerland, 2003

[3] ASTM, F1045-07 Standard Performance Specification for Ice Hockey Helmets. ASTM International, West Conshohocken, PA, USA, 2007.

[4] CSA, z262.1-09 Ice Hockey Helmets. Canadian Standards Association, Mississauga, Ontario, Canada, 2009.

[5] Mueller FO. Fatalities from head and cervical spine injuries occurring in tackle football: 50 years' experience. *Clin Sport. Med*, 1998, 17(1):169–182.

[6] Biasca N, Wirth S, Tegner Y. The avoidability of head and neck injuries in ice hockey: an historical review. *Br J Sport. Med*, 2002, 36(6):410–427.

[7] Rueda M F. Finite element modelling of equestrian helmet impacts exposes the need to address rotational kinematics in future helmet designs. *Comput. methods …*, 2011, 14(12):1021–1031.

[8] Post A, Walsh ES, Hoshizaki B, Gilchrist MD. Analysis of loading curve characteristics on the production of brain deformation metrics. *Proc. Inst. Mech. Eng. Part P J. Sport. Eng. Technol.*, 2012, 226(3/4):200-207.

[9] Bishop PJ, Arnold J. The effectiveness of hockey helmets in limiting localized loading on the head, in *Safety in Ice Hockey*, pp. 175–182, CR Castaldi, PJ Bishop, EF Horner (Eds), American Society for Testing Materials, Philadelphia, USA, 1993.

[10] Ouckama R, Pearsall DJ. Evaluation of a flexible force sensor for measurement of helmet foam impact performance. *J Biomech*, 2011, 44(5):904–909.

[11] Ouckama R, Pearsall DJ. Impact performance of ice hockey helmets: head acceleration versus focal force dispersion. *Proc. Inst. Mech. Eng. Part P J. Sport. Eng. Technol.*, 2012, 226(3-4):185–192.

[12] Halstead PD, Alexander CF, Cook EM, Drew RC. Hockey headgear and the adequacy of current designs and standards. *Saf. Ice Hockey Third Vol.*, 2000, 1341:93–100.

[13] McIntosh AS, Janda D. Evaluation of cricket helmet performance and comparison with baseball and ice hockey helmets. *Br J Sport. Med*, 2003, 37(4):325–330.

[14] Coulson NR, Foreman SG, Hoshizaki TB. Peak translational and rotational accelerations generated during reconstructed ice hockey impacts on a hybrid III headform. *Fifth Int. Symp. Saf. Ice Hockey*, 2008, 6(2).

[15] NHL, NHL Skills Competition All-Time Results, 1990-2011.: Internet: [http://www.nhl.com/ice/page.htm?id=67157] 2012, (Accessed 2012).

[16] Padgaonkar AJ, Krieger KW, King AI. Measurement of angular acceleration of a rigid body using linear accelerometers. *J. Appl. Mech.*, 1975, 42(3):552–556.

[17] DiMasi F. *Transformation of nine-accelerometer-package (NAP) data for replicating headpart kinematics and dynamic loading*. John A. Volpe National Transportation Systems Center: U.S. Department of Transportation, National Highway Traffic Safety Administration, 1995.

[18] Pellman EJ, Viano DC, et al. Concussion in professional football: helmet testing to assess impact performance--part 11. *Neurosurgery*, 2006, 58(1):78–96.

[19] SAE, *Instrumentation for Impact Test-Part 1: Electronic Instrumentation -SAEJ211-1*. Society of Automotive Engineers, Warrendale, PA, USA, 1995.
[20] Tekscan Inc, "Flexiforce Sensor User Manual (rev G)." Internet: [http://www.tekscan.com/pdfs/FlexiforceUserManual.pdf], 2009 (Accessed 2010).
[21] CSA, z262.6-09 Face protectors for use in ice hockey. Canadian Standards Association, Mississauga, Ontario, Canada, 2009.
[22] Takhounts EG, Ridella SA, et al. Investigation of traumatic brain injuries using the next generation of simulated injury monitor (SIMon) finite element head model. *Stapp Car Crash J*, 2008, 52:1–31.
[23] Hardy WN, Foster CD, et al. Investigation of head injury mechanisms using neutral density technology and high-speed biplanar x-ray. *Stapp Car Crash J*, 2001, 45:337–368.
[24] Nahum AM, Smith R, Ward CC. Intracranial pressure dynamics during head impact, *SAE Technical Paper 770922*, 1977.
[25] Trosseille X, Tarriere C, Lavaste F, Guillon F, Domont A. Development of a F.E.M. of the human head according to a specific test protocol. *Stapp Car Crash 36*, 1992, 36:235–253.
[26] Takhounts EG, Ridella SA, Rowson S, Duma SM. Kinematic rotational brain injury criterion (BRIC), *22nd International Technical Conference on the Enhanced Safety of Vehicles (ESV)*, 2011, 1–10.
[27] Yard EE, Comstock RD. Injuries sustained by pediatric ice hockey, lacrosse, and field hockey athletes presenting to United States emergency departments, 1990-2003. *J Athl Train*, 2006, 41(4):441–449.
[28] Zhang L, Yang KH, King AI. A proposed injury threshold for mild traumatic brain injury. *J Biomech Eng*, 2004, 126(2): 226–236.
[29] Walsh ES, Prost A, et al. Dynamic impact response characteristics of a helmeted Hybrid III headform using a centric and non-centric impact protocol. *Proc. Inst. Mech. Eng. Part P J. Sport. Eng. Technol.*, 2012, 226(3/4): 220-225.
[30] Viano DC, Casson IR, et al. Concussion in professional football: comparison with boxing head impacts--part 10. *Neurosurgery*, 2005, 57(6):1154–1172.
[31] Post A, Oeur A, Hoshizaki B, Gilchrist MD. Examination of the relationship between peak linear and angular accelerations to brain deformation metrics in hockey helmet impacts. *Comput. Methods Biomech. Biomed. Engin.*, 2011, 16(5): 511-519.
[32] Duma SM, Rowson S. Every newton hertz: A macro to micro approach to investigating brain injury. *Annual International Conference of the IEEE* Engineering in Medicine and Biology Society, 2009, Minneapolis, MN, USA, 1123–1126.
[33] Forero Rueda MA, Gilchrist MD. Computational analysis and design of components of protective helmets. *Proc. Inst. Mech. Eng. Part P J. Sport. Eng. Technol.*, 2012, 226(3/4):208–219.
[34] Brainard, L. L. et al., Gender Differences in Head Impacts Sustained by Collegiate Ice Hockey Players, *Medicine & Science in Sports & Exercise*, 2012, 44(2): 297–304.
[35] Nahum AM, Gatts JD, Gadd CW, Danforth J. Impact tolerance of skull and face, *Sae Trans.*, 1968, 77: 178.
[36] Raymond D, Van Ee C, Crawford G, Bir C. Tolerance of the skull to blunt ballistic temporo-parietal impact. *J Biomech*, 2009, 42(15):2479–2485.
[37] Sharkey EJ, Cassidy M, Brady J, Gilchrist MD, Nicdaeid N. Investigation of the force associated with the formation of lacerations and skull fractures. *Int. J. Legal Med.*, 2012, 126(6):835–844.
[38] Takhounts EG, Eppinger RH, et al. On the development of the SIMon finite element head model. *Stapp Car Crash J.*, 2003, 47:107–133.
[39] Yoganandan N, Pintar FA, Schlick M, Moore J, Maiman DJ. Comparison of head-neck responses in frontal impacts using restrained human surrogates. *Ann Adv Automot Med*, 2011, 55:181–191.